On the maximization of entropy in the process of thermalization of highly multimode nonlinear beams

Fabio Mangini, Mario Ferraro, Wasyhun Gemechu, Yifan Sun, Mikhail Gervaziev, Denis Kharenko, Sergey Babin, Vincent Couderc, Stefan Wabnitz

On the maximization of entropy in the process of thermalization of highly multimode nonlinear beams

Fabio Mangini,[1,†] Mario Ferraro,[2,†,*] Wasyhun A. Gemechu,[1,†] Yifan Sun,[1] Mikhail Gervaziev,[3,4] Denis Kharenko,[3,4] Sergey Babin,[3,4] Vincent Couderc,[5] and Stefan Wabnitz[1,3]

[1]Department of Information Engineering, Electronics, and Telecommunications, Sapienza University of Rome, Via Eudossiana 18, Rome 00184, Italy
[2]Physics Department, University of Calabria, Rende 87036, Italy
[3]Novosibirsk State University, Pirogova 1, Novosibirsk 630090, Russia
[4]Institute of Automation and Electrometry, SB RAS, Novosibirsk 630090, Russia
[5]Université de Limoges, XLIM, UMR CNRS 7252, 123 Avenue A. Thomas, Limoges 87060, France
[†]These authors contributed equally to this Letter.
*mario.ferraro92@unical.it

We present a direct experimental confirmation of the maximization of entropy which accompanies the thermalization of a highly multimode light beam, upon its nonlinear propagation in standard graded-index (GRIN) optical fibers.

https://doi.org/10.1364/OL.521563

The spatial beam self-cleaning effect consists of the nonlinear transformation of a multimode beam at the output of a multimode fiber (MMF) from speckles into a bell shape. This is typically observed in standard graded-index (GRIN) MMFs when the beam input power overcomes a certain threshold value [1–5]. The beam self-cleaning effect can be described in a thermodynamic framework: it represents the evolution of a disordered optical state toward a state of thermal equilibrium, or maximum entropy [6,7]. While the thermodynamic model cannot inherently encompass certain properties of self-cleaning, such as its preservation of spatial coherence and increase of beam brightness [1,8], which appear to be related to modal phase-locking mechanisms [9], mode-decomposition experiments have confirmed that indeed, as the input power grows larger, the output mode power distribution of self-cleaned beams approaches the Rayleigh–Jeans (RJ) law [10,11].

At first glance, it may seem counterintuitive that a self-cleaned bell-shaped beam contains more information than a beam with a seemingly chaotic speckled intensity distribution. This led to speculations that either the thermodynamic approach to multimode optical systems breaches the second law of thermodynamics or that the observed beam cleanup is due to the presence of some nonlinear dissipative effects [12].

Baudin *et al.* have experimentally determined the equilibrium entropy in the classical RJ condensation of light waves in an MMF [13]: in good quantitative agreement with the RJ theory [14], they found that the equilibrium entropy decreases with the internal energy of the beam (which corresponds to progressively higher values of fractional occupation of the fundamental fiber mode). In their experiments, the input power $\mathcal{P}$ is kept at constant, and the beam energy $\mathcal{U}$ is varied by controlling the spatial correlation of the speckle input beam with a diffuser. As a matter of fact, the thermodynamic theory considers $\mathcal{P}$ and $\mathcal{U}$ as constants of motion. However, in order to verify that beam self-cleaning is consistent with the second principle of thermodynamics, it is necessary to measure the entropy of out-of-equilibrium multimode states and verify that as thermal equilibrium is approached, the entropy indeed reaches a maximum value.

On the other hand, Ferraro *et al.* have demonstrated the validity of the second principle of thermodynamics for an ensemble of different optical multimode beams: in an optical calorimetry experiment, by using two orthogonally polarized beams at different temperatures (or internal energies), it was shown that heat flows from a *hot* to a *cold* beam and not vice versa [15]. As a result, the optical entropy grows larger in the process of heat exchange between the two beams. Incidentally, the growth of entropy accompanying the thermalization of a different highly multimode optical system, consisting of a photonic time-synthetic mesh lattice, has been recently reported [16].

In this work, we present the first experimental evidence of the growth of entropy in the thermalization of a single beam, an adiabatic process that is shown to occur in the absence of energy exchanges with the environment. Incidentally, it should be noted that wave thermalization in MMFs does not always lead to bell-shaped beams. Experiments have shown that, when increasing the beam power well above the self-cleaning threshold, a thermalized beam may still yield a speckled intensity pattern [17,18].

Let us provide first a simple theoretical proof that indeed the entropy of a highly multimode beam should always increase with power, in the process of transition from an out-of-equilibrium state to a state of thermal equilibrium. When propagating in a short length of the MMF, a multimode beam conserves its power $\mathcal{P} = \sum_i |c_i|^2$ and internal energy $\mathcal{U} = -\sum_i \beta_i |c_i|^2 = -\mathcal{P} \sum_i \beta_i |f_i|^2 \equiv \mathcal{P}u$, where $|c_i|^2$ ($|f_i|^2$) is the power (fraction)

carried by each mode ($i = 0, 1, \ldots M-1$). In GRIN fibers, the mode propagation constant β_i is supposed to be degenerate within each group of size $\lceil(\sqrt{1+8i}-1)/2\rceil$, where $\lceil\cdot\rceil$ is the ceiling function. The RJ mode power distribution

$$|c_i^{eq}|^2 = -\frac{T}{\mu+\beta_i} \tag{1}$$

is obtained from the condition of maximizing the Boltzmann entropy, which can be written as [6,19]

$$S = \sum_i^M \ln|c_i|^2, \tag{2}$$

where M is the number of the fiber modes. Here, the beam temperature T and chemical potential μ can be determined from the knowledge of $\mathcal{P}$ and U.

In typical practical experiments, the increase of entropy occurs at a fixed fiber length. Therefore, increasing $\mathcal{P}$ has the beneficial effect of facilitating the beam thermalization. Furthermore, beam cleanup is obtained by increasing $\mathcal{P}$, for a fixed injection condition of the laser into the fiber. This corresponds to maintaining a constant ratio between the internal energy and power, i.e., $u = const$. As such, by exploiting the equation of state $U - \mu\mathcal{P} = MT$ [6], we can write

$$\mu = \frac{U}{\mathcal{P}} - \frac{MT}{\mathcal{P}} = u - \frac{MT}{\mathcal{P}}, \tag{3}$$

which derived by $\mathcal{P}$ yields

$$\left(\frac{d\mu}{d\mathcal{P}}\right)_u = \frac{MT}{\mathcal{P}^2} - \frac{M}{\mathcal{P}}\left(\frac{dT}{d\mathcal{P}}\right)_u. \tag{4}$$

At thermal equilibrium, the entropy can be written as

$$S^{eq} = \sum_i \ln\left(-\frac{T}{\beta_i+\mu}\right) = M\ln(T) - \sum_i \ln(-\beta_i-\mu). \tag{5}$$

Now, by deriving S^{eq} by $\mathcal{P}$, it easily follows that

$$\left(\frac{dS^{eq}}{d\mathcal{P}}\right)_u = \frac{M}{T}\left(\frac{dT}{d\mathcal{P}}\right)_u - \sum_i \frac{1}{\beta_i+\mu}\left(\frac{d\mu}{d\mathcal{P}}\right)_u, \tag{6}$$

which recalling the definition of $\mathcal{P}$ and Eq. (4), leads to

$$\left(\frac{dS^{eq}}{d\mathcal{P}}\right)_u = \frac{M}{T}\left(\frac{dT}{d\mathcal{P}}\right)_u + \frac{\mathcal{P}}{T}\left(\frac{d\mu}{d\mathcal{P}}\right)_u = \frac{M}{\mathcal{P}} > 0, \tag{7}$$

i.e., the entropy at thermal equilibrium increases with power at $u = const$. This is sketched in Fig. 1(a) (black dashed curve), where we show a map of the values of S as a function of $\mathcal{P}$.

By definition, at fixed power $\mathcal{P}$ and internal energy U, the entropy at thermal equilibrium is maximal. Therefore, all values of S above the black dashed curve in Fig. 1(a) are inaccessible (nonphysical) states. The process of thermalization is illustrated by the red curve in Fig. 1(a): by increasing $\mathcal{P}$, a multimode system evolves from an out-of-equilibrium state A with an entropy S_A to a final state B which is at thermal equilibrium, i.e., it has an entropy $S_B = S^{eq}$. As it follows from the graph, since $S^{eq}(P)$ is a monotonically growing function, S must have a final value that is higher than its initial one, i.e., $S_B > S_A\ \forall$A. Still, it has to be noted that in its transient evolution toward thermal equilibrium, the entropy of a photon gas does not necessarily need to increase monotonically (as indicated by the oscillating red curve in Fig. 1(a)) [20]. In Fig. 1(b), we illustrate the relative mode power distribution of the fiber modes (which are considered for simplicity as populating the first four groups of degenerate modes only), corresponding to states labeled as A, A′, A″, and B in Fig. 1(a). Before presenting our experimental results, it is worth emphasizing that we compute the out-of-equilibrium entropy from the mode distributions by directly applying Eq. (2), which is valid at thermal equilibrium only. Nonetheless, our claim of entropy increase still holds, for it can be shown that S, as written in Eq. (2), provides an upper bound of the out-of-equilibrium entropy under the hypothesis that the fiber modes have Gaussian correlations (e.g., provided by random linear mode-coupling caused by a small variation of the refractive index) in addition to their individual fluctuations during pulse propagation within the fiber, leading to thermalization [19,21].

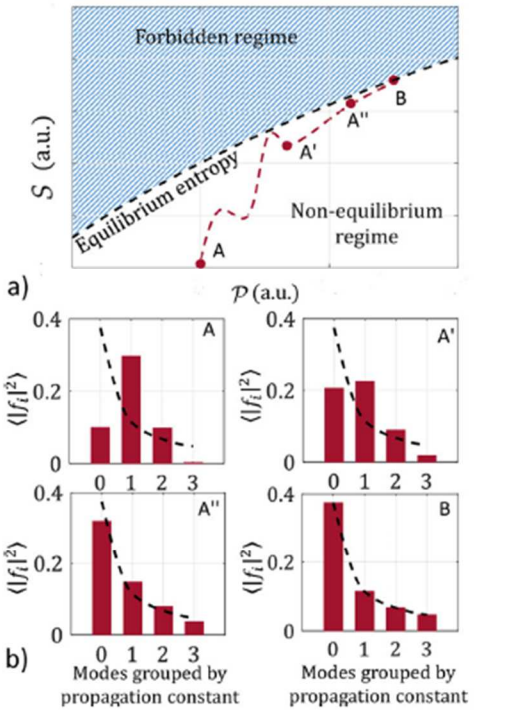

Fig. 1. (a) Illustration of beam trajectory from an out-of-equilibrium state A to an equilibrium state B via intermediate states A′ and A″, in the phase plane of optical entropy S versus beam power $\mathcal{P}$. (b) Normalized mean power fraction of the fiber modes grouped by the same propagation constant for states A, A′, A″, and B, respectively.

In our experiments, for giving a direct proof that the mode power distribution of a beam evolves toward a state of maximum entropy (i.e., it thermalizes), we kept the initial beam fixed and varied both the input power and the fiber length by means of a fiber cutback. A standard 12-m-long 50/125 GRIN MMF was coiled around a 15 cm diameter plastic drum, with a transparent tape securing the fiber every 2 m, for mitigating any undesired movement during the cutback procedure. The fiber output was directed onto a spatial light modulator through the combination of two confocal lenses. The near-field profile was subsequently imaged after being reflected from a flip mirror by using a CCD camera. The spatial light modulator reflection, corresponding to

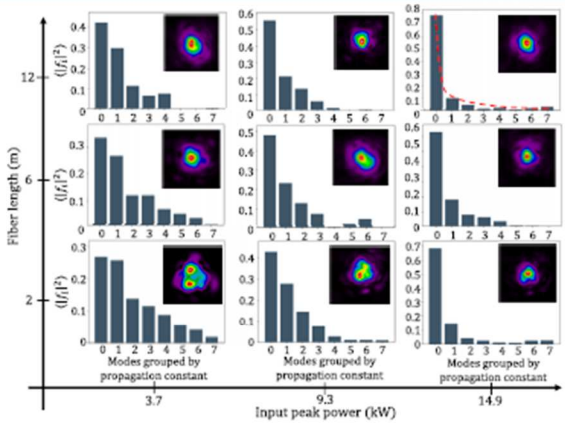

Fig. 2. Normalized mean power fraction of fiber modes (grouped by their propagation constant) versus the fiber length and the input peak power, respectively. Insets show the corresponding measured near-field intensities.

the Fourier transform of the output beam, was imaged by another camera after passing through a convex lens. To counteract the loss of temporal coherence resulting from self-phase modulation (SPM), a bandpass filter was introduced into the optical path. We verified that no significant power-dependent loss was introduced by the presence of the filter, meaning that the effects of SPM can be neglected [17]. Additionally, a half-wave plate and a linear polarizer were incorporated to control the intensity and linear polarization state of the output beam on the spatial light modulator; for more details on the mode decomposition (MD) method, we refer to Ref. [11,22].

Figure 2 summarizes the results of our MD experiments: here we show the variation of the output mode power distribution when either the input power or the fiber length are varied, respectively. We report the normalized mean power fraction of the fiber modes, according to their degeneracy group. One can appreciate that, when moving in both directions, an RJ distribution (see red dashed line in the top right panel of Fig. 2) is always approached. This underlines the fact that beam thermalization can be obtained by increasing either the input power or the propagation distance. Moreover, the RJ distribution has a dominant (>70%) contribution from the fundamental mode of the GRIN fiber, which leads to the characteristic bell-shaped transverse intensity profile of a self-cleaned beam.

Now, the Boltzmann entropy S can also be written as

$$S = M \ln \mathcal{P} + \sum_{i=1}^{M} \ln |f_i|^2. \tag{8}$$

In the experiments, we have isolated the contribution of the second term in Eq. (8):

$$\tilde{S} = \sum_{i=1}^{M} \ln |f_i|^2, \tag{9}$$

which only implicitly depends on the input power $\mathcal{P}$, through the nonlinear change of the mode power distribution. As such, we will refer to $\tilde{S}$ as *the configuration entropy* (or the entropy per particle as in [15]). $\tilde{S}$ is a useful parameter to estimate in our experiments because it increases with $\mathcal{P}$ and reaches a steady-state value whenever thermal equilibrium is achieved. Since the first term in Eq. (8) is proportional to the input power, if we can demonstrate that $\tilde{S}$ grows larger toward a maximal value as the out-of-equilibrium beam tends toward thermalization, then the Boltzmann entropy S is also maximized necessarily when approaching S^{eq}. Note that when $u = const$ as it occurs in our experiments, Eq. (7) predicts that $\tilde{S}^{eq} = const$: in order words, at thermal equilibrium—i.e., for sufficiently long fibers or high input powers—the contribution to the entropy from the mode power distribution is independent of input power.

Before presenting our results, it is worth remarking that our MD tool has limited accuracy when measuring the population of higher-order modes (HOMs). As a result, it may occur that the measured power fraction of some HOMs is nearly vanishing. This can be easily anticipated, given that the power fraction of HOMs progressively decreases, as their mode order grows larger, according to the RJ law (1) at thermal equilibrium. Now, a value of $c_i = 0$ makes the logarithmic term in Eq. (9) diverging. When measuring the entropy, this may result in a significant limitation to its accuracy, unless a proper data regularization is applied. We circumvented this issue by introducing a threshold value for the mode power fraction, as already discussed in detail in Refs. [7,15]. Specifically, here has been set to zero the power of HOMs such that $|f_i|^2 < 0.032$. Such a stratagem, which is largely justified by the limited accuracy of our holographic MD tool, allows us to strongly reduce measurement fluctuations when evaluating the entropy.

Our experimental findings about the evolution of the configuration entropy $\tilde{S}$ are summarized in Fig. 3. In the first set of experiments (see Fig. 3(a)), we measured the increase of entropy of the output beam from a fixed length of the MMF, when

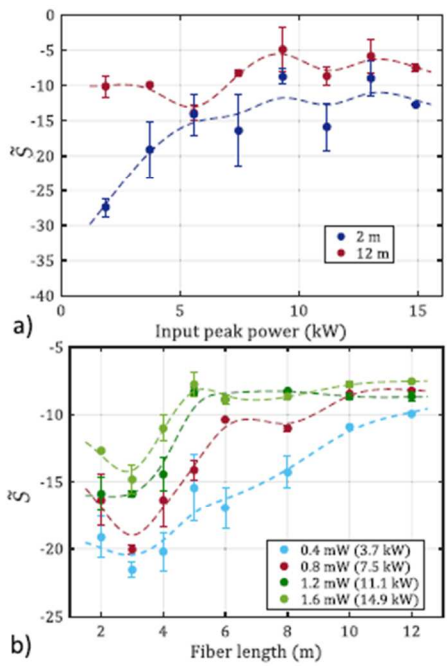

Fig. 3. (a) Variation of the beam entropy versus the input peak power for fiber lengths of 2 (blue line) and 12 m (red line). (b) Variation of the beam entropy versus the fiber length for different input beam powers (the legend shows the average and the peak power of the optical pulses, respectively). Dashed curves are guides for the eye.

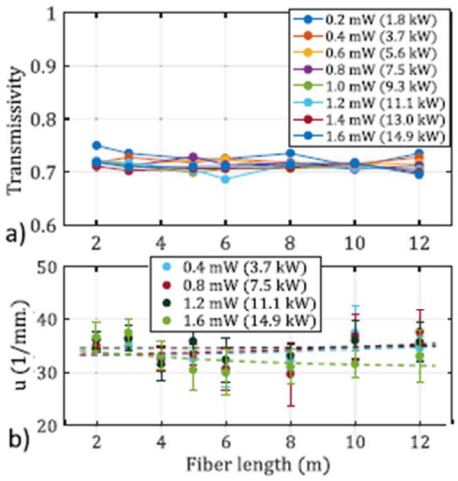

Fig. 4. Conservation of the beam power (a) and normalized energy u (b) versus the fiber length, for different input beam powers; the legends show the average and the peak power of the optical pulse trains, respectively.

increasing the input power above the self-cleaning power threshold. Note that when out-of-equilibrium states are concerned, oscillations in the evolution of both S and $\tilde{S}$ are possible.

It is interesting to note from Fig. 3(a) that for the shorter fiber length (2 m), a clear increase of $\tilde{S}$ is observed as the input power is first increased up to 5 kW: at higher powers, the configuration entropy tends to saturate, as it is expected when the beam is nearly thermalized. Figure 3(a) also shows that at the longest length (12 m), the evolution of $\tilde{S}$ with power exhibits oscillations superimposed on a relatively slow growth, which indicates that the multimode gas is relatively close to its state of equilibrium for all power values.

Next, we fixed the input power and carried out a series of cutback experiments, which permitted us to monitor the evolution of $\tilde{S}$ along the propagation distance in the fiber (which plays the role of evolution time of the photon gas). Note that in this particular case, it is fully equivalent to study the evolution of S or $\tilde{S}$, since the input power is fixed and the second term in Eq. (8) remains a constant. As can be seen in Fig. 3(b), $\tilde{S}$ exhibits a general trend of growing larger with distance. Consistently with the results of Fig. 3(a), for the lowest peak power value of 3.7 kW (light blue dots and dashed curve), a rapid growth of $\tilde{S}$ over the first 6 m is observed, followed by a saturation of its growth with distance, again as expected when thermal equilibrium is reached. On the other hand, at the highest peak power of 14.9 kW, for lengths longer than 4 m, $\tilde{S}$ remains essentially flat since at this high power level, thermalization is achieved at shorter distances.

Finally, we verified the pillars on which the thermodynamic theory relies, i.e., the conservation of $\mathcal{P}$ and u: this is shown in Fig. 4). Figure 4(a) shows that the power transmissivity of the fiber itself is essentially determined by input coupling loss. As can be seen, the transmissivity remains essentially constant at all lengths and for all power levels, which rules out the possible presence of dissipative effects in determining the beam self-cleaning. In addition, Fig. 4(b) demonstrates the invariance of the normalized internal energy u at all propagation distances and for all tested power values.

In conclusion, multimode fiber cutback studies combined with mode decomposition experiments could provide a direct experimental demonstration that the mode power distribution associated with a self-cleaned state evolves toward a global maximum of optical entropy, which indicates that the optical field has reached a state of thermal equilibrium.

Funding. Horizon Europe Marie Sklodowska-Curie Actions (101023717, 101064614); Sapienza Università di Roma (RG12117A84DA7437); NRRP of NextGenerationEU (PE00000001 - "RESTART"); Agence Nationale de la Recherche (ANR-10-LABX-0074-01, ANR-18-CE080016-01); Russian Science Foundation (21-72-30024); Italian Ministry of University and Research (MUR) PRIN 2022 "SAFE2" (2022ESAC3K).

Acknowledgment. We thank G. Steinmeyer, A. Picozzi, F. Wise, F.O. Wu, and D.N. Christodoulides for their fruitful discussions.

Disclosures. The authors declare no conflicts of interest.

Data availability. Data underlying the results presented in this paper are not publicly available at this time but may be obtained from the authors upon reasonable request.

REFERENCES

1. K. Krupa, A. Tonello, B. M. Shalaby, *et al.*, Nat. Photonics **11**, 234 (2017).
2. K. Krupa, A. Tonello, A. Barthélémy, *et al.*, Phys. Rev. Lett. **116**, 183901 (2016).
3. Z. Liu, L. G. Wright, D. N. Christodoulides, *et al.*, Opt. Lett. **41**, 3675 (2016).
4. L. G. Wright, Z. Liu, D. A. Nolan, *et al.*, Nat. Photonics **10**, 771 (2016).
5. E. Podivilov, F. Mangini, O. Sidelnikov, *et al.*, Phys. Rev. Lett. **128**, 243901 (2022).
6. F. O. Wu, A. U. Hassan, and D. N. Christodoulides, Nat. Photonics **13**, 776 (2019).
7. M. Ferraro, F. Mangini, M. Zitelli, *et al.*, Adv. Phys.: X **8**, 2228018 (2023).
8. M. Fabert, M. Săpânţan, K. Krupa, *et al.*, Sci. Rep. **10**, 20481 (2020).
9. F. Mangini, M. Ferraro, Y. Sun, *et al.*, Opt. Lett. **48**, 3677 (2023).
10. H. Pourbeyram, P. Sidorenko, F. O. Wu, *et al.*, Nat. Phys. **18**, 685 (2022).
11. F. Mangini, M. Gervaziev, M. Ferraro, *et al.*, Opt. Express **30**, 10850 (2022).
12. G. Steinmeyer, in *CLEO/Europe-EQEC* (IEEE, 2023), p. 1.
13. K. Baudin, A. Fusaro, K. Krupa, *et al.*, Phys. Rev. Lett. **125**, 244101 (2020).
14. P. Aschieri, J. Garnier, C. Michel, *et al.*, Phys. Rev. A **83**, 033838 (2011).
15. M. Ferraro, F. Mangini, F. Wu, *et al.*, Phys. Rev. X **14**, 021020 (2024).
16. A. Marques Muniz, F. Wu, P. Jung, *et al.*, Science **379**, 1019 (2023).
17. F. Mangini, M. Ferraro, A. Tonello, *et al.*, Opt. Lett. **48**, 4741 (2023).
18. K. Baudin, J. Garnier, A. Fusaro, *et al.*, Phys. Rev. Lett. **130**, 063801 (2023).
19. K. G. Makris, F. O. Wu, P. S. Jung, *et al.*, Opt. Lett. **45**, 1651 (2020).
20. A. Picozzi, Opt. Express **15**, 9063 (2007).
21. O. S. Sidelnikov, E. V. Podivilov, M. P. Fedoruk, *et al.*, Opt. Fiber Technol. **53**, 101994 (2019).
22. M. D. Gervaziev, I. Zhdanov, D. S. Kharenko, *et al.*, Laser Phys. Lett. **18**, 015101 (2021).